Received: 5 June 2023 | Revised: 17 July 2023 | Accepted: 23 July 2023

DOI: 10.1002/bit.28523

ARTICLE

BIOTECHNOLOGY AND BIOENGINEERING WILEY

Thermostability enhancement of polyethylene terephthalate degrading PETase using self- and nonself-ligating protein scaffolding approaches

Barindra Sana[1] | Ke Ding[1] | Jia Wei Siau[1] | Rupali Reddy Pasula[2] | Sharon Chee[1] | Sharad Kharel[3] | Jean-Baptise Henri Lena[3] | Eunice Goh[4] | Lakshminarayanan Rajamani[4] | Yeng Ming Lam[3] | Sierin Lim[2] | John F. Ghadessy[1]

[1]Disease Intervention Technology Laboratory, Institute of Molecular and Cell Biology, Agency for Science Technology and Research, Singapore, Singapore

[2]School of Chemistry, Chemical Engineering and Biotechnology, Nanyang Technological Univeristy, Singapore, Singapore

[3]School of Materials Science and Engineering, Nanyang Technological University, Singapore, Singapore

[4]Singapore Eye Research Institute, The Academia, Singapore, Singapore

Correspondence
John F. Ghadessy.
Email: fghadessy@imcb.a-star.edu.sg

Funding information
National Research Foundation Singapore

Abstract

Polyethylene terephthalate (PET) hydrolase enzymes show promise for enzymatic PET degradation and green recycling of single-use PET vessels representing a major source of global pollution. Their full potential can be unlocked with enzyme engineering to render activities on recalcitrant PET substrates commensurate with cost-effective recycling at scale. Thermostability is a highly desirable property in industrial enzymes, often imparting increased robustness and significantly reducing quantities required. To date, most engineered PET hydrolases show improved thermostability over their parental enzymes. Here, we report engineered thermostable variants of *Ideonella sakaiensis* PET hydrolase enzyme (*Is*PETase) developed using two scaffolding strategies. The first employed SpyCatcher-SpyTag technology to covalently cyclize *Is*PETase, resulting in increased thermostability that was concomitant with reduced turnover of PET substrates compared to native *Is*PETase. The second approach using a GFP-nanobody fusion protein (vGFP) as a scaffold yielded a construct with a melting temperature of 80°C. This was further increased to 85°C when a thermostable PETase variant (FAST PETase) was scaffolded into vGFP, the highest reported so far for an engineered PET hydrolase derived from *Is*PETase. Thermostability enhancement using the vGFP scaffold did not compromise activity on PET compared to *Is*PETase. These contrasting results highlight potential topological and dynamic constraints imposed by scaffold choice as determinants of enzyme activity.

KEYWORDS
engineering, hydrolase, PET, scaffold, thermostability, vGFP

Barindra Sana, Ke Ding, and Jia Wei Siau contributed equally to this study.

1 | INTRODUCTION

Ever-increasing demand and indiscriminate use of single-use plastics have created a worldwide pollution problem, with growing amounts of plastic waste accumulating in landfills and natural environments including marine and terrestrial ecosystems. While nondegradability and durability are great advantages of plastic materials, they lead to major environment pollution from cumulative plastic waste. Around 33 billion tons of discarded plastics will accumulate on earth by 2050 (Rochman et al., 2013). Polyethylene terephthalate (PET) is one of the most abundant plastics with estimated global production of 70 million tons annually (Tournier et al., 2020), and is widely used in disposable containers for many commercial foods and drinks. Therefore, much effort has been employed to recycle PET waste. Thermal, chemical, and mechanical processes have been described for this purpose (Kijo-Kleczkowska & Gnatowski, 2022). These are generally not eco-friendly and often require high temperatures, organic solvents, hazardous chemicals, and high energy consumption. Some of these recycling processes also cause loss of mechanical properties that ultimately limits the life cycle of PET polymers (Itim & Philip, 2015).

In recent years, several microbial enzymes have been reported to hydrolyze PET, albeit with low efficiencies on highly crystalline substrates such as nonpretreated commercial-grade PET bottles (Kawai et al., 2014; Müller et al., 2005; Sulaiman et al., 2012; Yoshida et al., 2016). Significant enzyme engineering is therefore being undertaken to improve activities of these enzymes (Cui et al., 2021; Lu et al., 2022; Tournier et al., 2020). Tournier et al. reported an engineered cutinase enzyme with optimal activity at 72°C that more efficiently hydrolyzes PET to its monomer (Tournier et al., 2020). This thermostable enzyme is being commercialized by the French biotech company Carbios (Thiyagarajan et al., 2022). *Ideonella sakaiensis*, a bacterium isolated from a plastic bottle recycling plant secretes *Is*PETase, a PET hydrolyzing enzyme that shows relatively high intrinsic PET-degrading activity (Yoshida et al., 2016). Numerous engineered *Is*PETase (hereafter referred to as PETase) variants have been described with improved activities (Austin et al., 2018; Bell et al., 2022; Joho et al., 2023; Joo et al., 2018; Liu et al., 2018; Meng et al., 2021; Rennison et al., 2021; Samak et al., 2020; Shi et al., 2023; Son et al., 2020; Yin et al., 2022; Zurier & Goddard, 2023). Notably, most of these show enhanced thermostability over wild-type PETase. Son et al. described a thermostable PETase mutant with 14-fold higher PET degradation activity at 40°C compared to the wild-type enzyme (Son et al., 2019). The more efficient Dura- and FAST-PETase variants were developed using computational design and machine learning strategies, respectively. DuraPETase (Cui et al., 2021) comprises 10 mutations and its melting temperature (T_m) of 77°C is 31°C higher the wild-type PETase. FAST PETase (Lu et al., 2022) (five mutations) displays enhanced hydrolysis of PET substrates with varying degrees of crystallinity at 50°C and has a T_m of 67.1°C.

Given this apparent association of enhanced activity with thermostability, we sought to further engineer the latter using alternative scaffolding approaches (Lau et al., 2018; Sana et al., 2019; Woodman et al., 2005) in lieu of direct mutation. Our first strategy employed the self-ligating SpyCatcher (SC)-SpyTag (ST) scaffold (Li et al., 2014) to cyclize PETase. We next used the thermostable vGFP construct previously shown to effectively scaffold and present exogenous bioactive peptides (Chee et al., 2021). While both approaches yielded thermostable PETase variants, SC-ST cyclization resulted in a reduced activity on PET substrate not observed for the vGFP scaffold. The differing scaffold topologies likely impact enzyme dynamics to account for the observed phenotypes.

2 | MATERIALS AND METHODS

2.1 | Cloning and mutation

The *Is*PETase gene was codon-optimized for recombinant expression in *Escherichia coli* and synthesized (IDT). The gene was amplified using primers 1a and 1b (see Supporting Information: Table S1 for list of oligonucleotide primers). The purified PCR product was cloned with a C-terminus 6-His tag into pET22b vector via NdeI/XhoI using the In-Fusion HD Cloning kit following the manufacturer's protocol (Takara bio). The construct was transformed into chemically competent *E. coli* DH5α cells (Invitrogen) and the correct sequence was confirmed by sequencing.

The cPETase (SC-*Is*PETase-ST) construct was made by inserting the *Is*PETase gene cassette into a SC-10His-linker-ST construct (inserted between NdeI and BamHI sites of pET22b vector). The construct was linearized by inverse PCR using primers 2a and 2b, and the *Is*PETase gene was amplified using primers 3a and 3b. Correct-sized bands from the PCR products were gel extracted. The amplified *Is*PETase gene was inserted in the linearized vector by In-Fusion cloning as described above.

The mcPETase construct was made by introducing D383G point mutation in the cPETase construct by PCR, using primers 4a and 4b. The PCR product was digested using DpnI enzyme to remove parental templates and transformed into chemically competent *E. coli* DH5α cells (Invitrogen).

The c2PETase construct was made by inserting the GGGGS linker at N-terminus of the PETase gene in the cPETase construct. The insertion was done by PCR using 5a and 5b primers; the PCR product was DpnI digested, gel extracted, and ligated by intra-molecular ligation. Chemically competent *E. coli* DH5α cells (Invitrogen) were transformed with 1 µL ligation product and the correct construct was selected after sequencing.

The gene encoding PETase enzyme was inserted in frame into the linker region connecting the eGFP and the nanobody (NB) enhancer component of vGFP (Eshaghi et al., 2015) to make eGFP-PETase-NB construct. The vGFP construct in pET22b vector was linearized by inverse PCR using primers 6a and 6b. The PCR product was DpnI digested and the correct-sized band was purified after agarose gel electrophoresis. The PETase gene was amplified by PCR using primers 7a and 7b. The PCR product was gel purified and inserted in the linearized vGFP construct by infusion cloning. The sequence of the resulting eGFP-PETase-NB (or vGFP-PETase or vPETase) construct was confirmed by DNA sequencing.

Two truncated vGFP constructs were made by removing the eGFP or the NB from the vPETase constructs. The eGFP was removed by inverse PCR of the vPETase constructs using primers 8a and 8b, while the NB component was removed by inverse PCR of the vPETase constructs using primers 9a and 9b. The PCR products were DpnI digested; the correct-sized bands were gel purified and circularized by intramolecular ligation.

Construct amino acid sequences are shown in Supporting Information: Table S2.

2.2 | Recombinant protein expression and purification

Plasmid constructs of PETase variants were transformed into *E. coli* SHuffle T7 competent cell following the manufacturer's protocol (New England Biolabs) and grown on LB-agar plates containing 0.1 mg/mL ampicillin at 30°C for 2 days. Overnight cultures were prepared by inoculating single colonies in LB broth containing 0.1 mg/mL ampicillin and grown at 30°C with constant shaking. For overexpression, the overnight cultures were diluted 100-fold in the same media, grown at 30°C until OD600 0.5, and induced with 0.5 mM IPTG. The culture was grown at 16°C for 20 h.

The proteins were purified using Ni-NTA column (GE healthcare) following manufacturer's protocol. The purified proteins were concentrated and buffer exchanged into PBS using 10 kDa MWCO Amicon Ultra centrifugal filters. The concentration and purity of the purified proteins were determined by OD280 using Nanodrop and SDS-PAGE, respectively.

2.3 | PNPA enzyme assay

Enzymes were assayed colorimetrically using para nitrophenyl acetate (PNPA) as substrate. Reactions (in triplicate) comprised enzyme (50 nM), PNPA (0.5 mM) in PBS buffer (total volume 100 µL). After incubation at 37°C, absorbance was measured at 405 nm using PBS as blank. For thermal stability studies,100 µL samples of 3.6 µM purified PETase in PBS were heated in a thermocycler over the required temperature range for 10 min. The samples were cooled on ice and the soluble fraction obtained via centrifugation at 13,000 rpm for 30 min at 4°C. Enzymes were assayed colorimetrically using PNPA as substrate. For each reaction, 10 µL of the soluble fraction was added to a 90 µL reaction containing 80 µL PBS and 10 µL of 5 mM PNPA stock (in absolute ethanol), and the reaction incubated at 37°C for 10 min. The absorbances at 405 nm were measured immediately via Envision plate reader. Blanks were made without adding any enzyme. Biological duplicates were carried out, with each replicate having technical duplicates. A total of 13 µL of the soluble fractions were further made up to 20 µL with 4× LDS sample buffer and 10× reducing agent, heated at 95°C for 10 min and 15 µL analyzed by SDS-PAGE.

2.4 | Circular dichroism (CD) and melting temperature study

Circular dichroism (CD) measurements were performed on a ChirascanTM CD spectrophotometer (Applied Photophysics) with a temperature control unit. Protein samples were diluted to 0.2 mg/mL with buffer (50 mM Na_2HPO_4, pH 8.0, 100 mM NaCl) and the CD spectra were recorded between 30–55/80°C (heating and cooling), between 190 and 260 nm (in 1 nm steps), using a quartz cuvette with a path length of 1 mm.

2.5 | Kinetics study

The enzyme activities were measured using 50, 75, 100, 125, 150, 200, and 250 µM PNPA as substrate in PBS at room temperature (chamber temperature 22.6 ± 0.2°C). The substrates were premixed with the buffer and the reactions were started by mixing with 0.36 µM of the respective enzyme inside individual wells of a 384-well plate, with total reaction volume of 100 µL. Progress of the reactions was monitored by measuring absorbance at 405 nm at 10 s intervals (for production of para-nitrophenol) using a plate reader (Envision, Perkin-Elmer). All experiments were conducted in triplicate, and kinetic data were calculated using the Lineweaver–Burk Plot. The product concentrations were calculated using 18,000 M^{-1} cm^{-1} as the extinction coefficient of para-nitrophenol at 405 nm.

2.6 | Differential scanning fluorimetry (thermofluor) assay

A 12.5× stock solution was made by diluting 5000× SYPRO orange protein gel stain (Invitrogen) in PBS; 5 µL of the diluted solution was taken into PCR tubes and mixed with 45 µL of protein (5 µM stock of PETase variants). The mixture was incubated at RT for 20 min and then assayed in the qPCR machine, using HEX channel. The fluorescence measurements were done at every 0.5°C increment of temperature, from 25°C to 95°C. The melting temperatures were calculated from the melt-curves using automated function on PCR machine (BioRad CFX96).

2.7 | Enzymatic PET hydrolysis

PET powder (<106 µm particle size) was prepared by grinding commercially available PET film (Goodfellow, catalog # ES301445). A total of 1 mg of this PET powder was mixed with 100 µL buffer (200 mM phosphate buffer pH 8.0) and 200 nM enzyme. The final volume was made up to 200 µL with water and reactions incubated at 30, 37, or 50°C for 3 days. The reaction was terminated by heating at 95°C for 10 min, and the insoluble fractions were removed by centrifuging at 13,500*g* for 10 min. A total of 100 µL supernatants were mixed with equal volume of DMSO and analyzed by HPLC using

an Eclipse Plus C18, 4.5 × 150 mm, 5 µm column (Agilent Technologies) in an Agilent 1260 HPLC system equipped with a DAD detector. Mobile phase A comprised of 1% formic acid (Sigma Aldrich) and mobile phase B comprised of acetonitrile (Sigma Aldrich). Flowrate of 1 mL/min with a sample volume of 10 µL was detected at 260 nm wavelength. Terephthalic acid (TPA), mono-(2-hydroxyethyl) terephthalate (MHET), and bis(2-hydroxyethyl) terephthalate (BHET) were separated with a gradient of 15%–35% acetonitrile over 8 min following which the column was flushed with 50% Acetonitrile for 1 min and conditioned at 15% acetonitrile for 5 min. Standard plots of TPA (Sigma-Aldrich), MHET (Amatek Chemicals), and BHET (Sigma-Aldrich) were obtained from area-under-curve of the corresponding HPLC peak using which amount of PET degraded in the enzymatic reaction and percentage PET degradation was subsequently calculated. Representative HPLC separation chromatogram, standard plots and raw data shown in Supporting Information: Figure S10, Supporting Information: Tables S3, S4.

3 | RESULTS

3.1 | Enhanced PETase thermostability by SC-ST cyclization

PETase was first scaffolded using SC-ST technology (Zakeri et al., 2012). ST is a short peptide that spontaneously forms an isopeptide bond with its binding partner SC protein. When a protein of interest is scaffolded by the respective appendage of SC and ST components to its N- and C-termini, spontaneous amide bonding between the termini results in cyclization. This strategy has been used to develop several cyclic thermostable enzymes (Schoene et al., 2014; Si et al., 2016; Wang et al., 2016). PETase is an ideal candidate for SC-ST-mediated cyclization considering the short distance between the two termini and their nonproximity to its active site (Figure 1). We first expressed and purified a construct comprising SC-PETase-ST (cPETase) in addition to PETase (Supporting Information: Table S2). Thermostability was assessed by heating proteins for 10 min over a 20–90°C temperature range and measuring residual activity (postcentrifugation to remove insoluble precipitate) using the model colorimetric substrate PNPA. cPETase was more thermostable than PETase, retaining 37% activity after 10 min incubation at 90°C, whereas PETase lost all activity at incubation temperatures >55°C (Figure 2a). SDS-PAGE analysis of the same samples confirmed enhanced thermostability of cPETase up to 80°C, while PETase completely denatured and precipitated above 50°C incubation temperatures (Figure 2b, Supporting Information: Figure S1). The T_m of PETase determined by ThermoFluor assay (Matulis et al., 2005) was 43.5°C, in agreement with previous studies (Fecker et al., 2018) (Figure 3). cPETase showed a biphasic melting profile with T_ms of 44.5°C and 76.5°C (Figure 3). The first T_m corresponds to PETase domain unfolding, while the second peak likely derives from unfolding of the SC domain thermostabilized by covalently bound ST (Siau et al., 2020). A similar observation has been reported for SC-ST mediated cyclization of β-lactamase enzyme (Schoene et al., 2014), indicating that the scaffold is likely promoting refolding of PETase upon heat-denaturation instead of increasing resistance to unfolding. To verify that the increased thermostability is due to covalent cyclization of PETase, we mutated a crucial aspartic acid residue in ST responsible for formation of the isopeptide bond to a lysine reside in SC (Zakeri et al., 2012). This D383G mutant cPETase (mcPETase) showed a T_m of 45°C, similar to that of PETase. Furthermore, the higher-temperature melt peak observed in cPETase was absent for mcPETase.

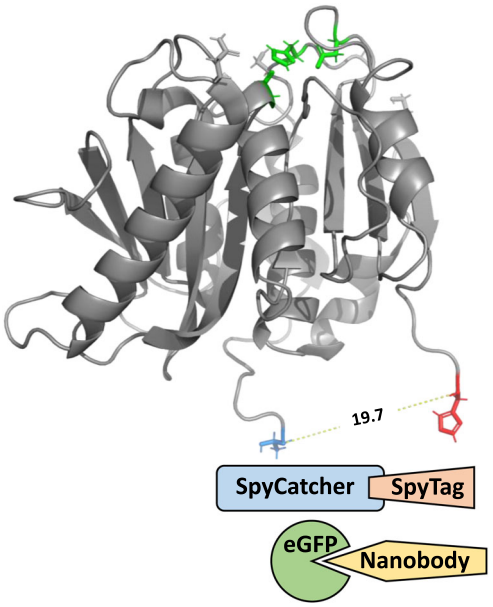

FIGURE 1 Crystal structure of *Is*PETase showing the distance (angstroms) between N and C termini (terminal residues respectively depicted blue and red). The catalytic triad residues are shown in green. Respective N and C termini fusion positions of SpyCatcher/SpyTag and eGFP/nanobody pairs also depicted. *Is*PETase, *Ideonella sakaiensis* PET hydrolase enzyme. Adapted from PDB ID: 6eqe (Austin et al., 2018).

3.2 | Enzymatic activities of PETase and cPETase

Kinetics studies were carried out using PNPA substrate. The K_m of PETase was 1.98 ± 0.1 mM, comparable to previously reported values (Fecker et al., 2018). The catalytic efficiency (k_{cat}/K_m) of cPETase was approximately 10 times lower than that of PETase (Table 1). This resulted from both reduced k_{cat} (4-fold) and lower binding affinity (2.5-fold). We hypothesized that cPETase had compromised enzymatic activity due to conformational constraints imposed by cyclization. Extending linker length (insertion of GGGGS) between SC and PETase yielded the c2PETase variant (Supporting Information: Table S2) with 17-fold increase in k_{cat}/K_m over cPETase and 1.8-fold increase over PETase for PNPA turnover. The increase was largely driven by improved affinity for PNPA substrate. This variant showed similar thermostability to cPETase (Figures 2a,b, 3). Activity

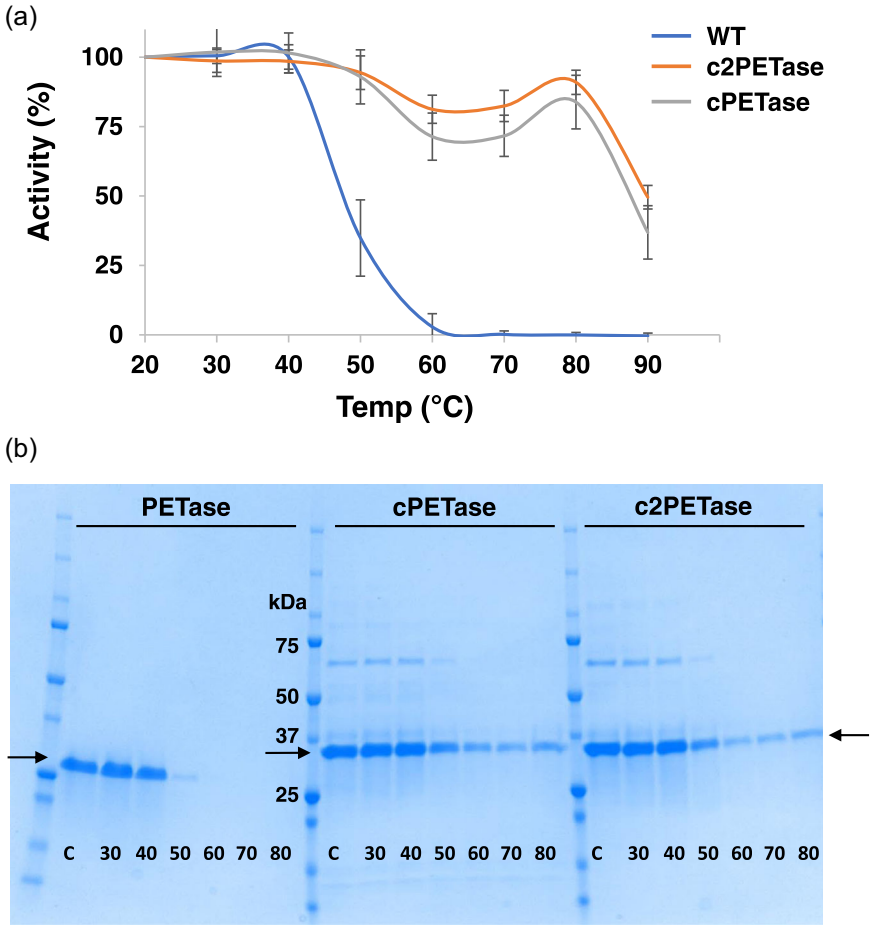

FIGURE 2 (a) Activity on para nitrophenyl acetate substrate of heat-treated PETase (blue), cPETase (gray) and c2PETase (orange) after heating purified proteins for 10 min at indicated temperatures. $n = 4 \pm$ SD. (b) Enzyme thermostability measured by SDS PAGE. Enzymes were incubated at indicated temperatures for 10 min and denatured/precipitated proteins removed by centrifugation. Soluble proteins were visualized by SDS PAGE. (c) control (unheated). Arrows represent proteins of expected size. Repeat data in Supporting Information: Figure S1.

of c/c2PETase variants was next measured using a low crystallinity (8%) PET powder substrate with particle size <106 µm (Supporting Information: Figure S2). cPETase showed ~10-fold reduced PET hydrolysis, similar to the reduced activity seen on PNPA. Activity of c2PETase was also notably lower (~ 5-fold) than PETase after 3 days incubation at 30°C and 37°C (Figure 4).

3.3 | Enhanced PETase thermostability by vGFP scaffolding

We next investigated the use of vGFP as a scaffold to potentially thermostabilize PETase. vGFP comprises eGFP N-terminally fused to an exceptionally high-affinity NB binder by a peptide linker (Eshaghi et al., 2015). We have previously demonstrated scaffolding of bioactive peptides into the linker region to effectively display them in a "pseudo-cyclised" conformation for imaging and biosensing applications (Chee et al., 2021). Given the inherent thermostability of vGFP (T_m of 89°C) we therefore asked if it could scaffold larger inserts such at PETase. A construct comprising eGFP-PETase-NB (vGFP-PETase) was expressed and purified along with controls (eGFP-PETase, PETase-NB) (Supporting Information: Table S2). These were preincubated for 10 min over a range of temperatures before measurement of PNPA hydrolysis. In the absence of thermal insult, vGFP-PETase showed similar enzymatic activity to PETase. However, it was considerably more thermostable, retaining ~ 50% activity after incubation at 80°C. (Figure 5a). Control proteins lacking either eGFP or NB showed similar thermostability to PETase. We further explored vGFP scaffolding of the FAST PETase variant engineered for both thermostability and improved PET degradation activity (Lu et al., 2022). As expected, FAST alone showed ~10°C improved thermostability over PETase. vGFP-FAST showed ~5°C improved thermostability over vGFP-PETase, with a T_m of 85°C.

SDS-PAGE analysis of soluble protein after heat treatment and centrifugation to remove precipitates confirmed the enhanced thermostability of vGFP-PETase over PETase and the controls (Figure 5b). Incubation at higher temperatures showed near binary total loss of protein at incubation temperatures above 80°C and 85°C for vGFP-PETase and vGFP-FAST, respectively (Figure 5c), indicating a marked buffering capacity of vGFP with regard to maintaining solubility of the scaffolded PETase cargo. Visual inspection also showed increased retention of eGFP fluorescence in vGFP-PETase and vGFP-FAST compared to eGFP-PETase control postheating (Figure 6).

As with SC-ST cyclisation, the T_m of the PETase component of vGFP-PETase measured using thermofluor assay was very similar to that of PETase (45°C vs. 44.5°C) (Figure 7a). FAST alone displayed a T_m of 60°C using thermofluor. As with PETase, the T_m of the FAST component in vGFP-FAST did not appear to change significantly

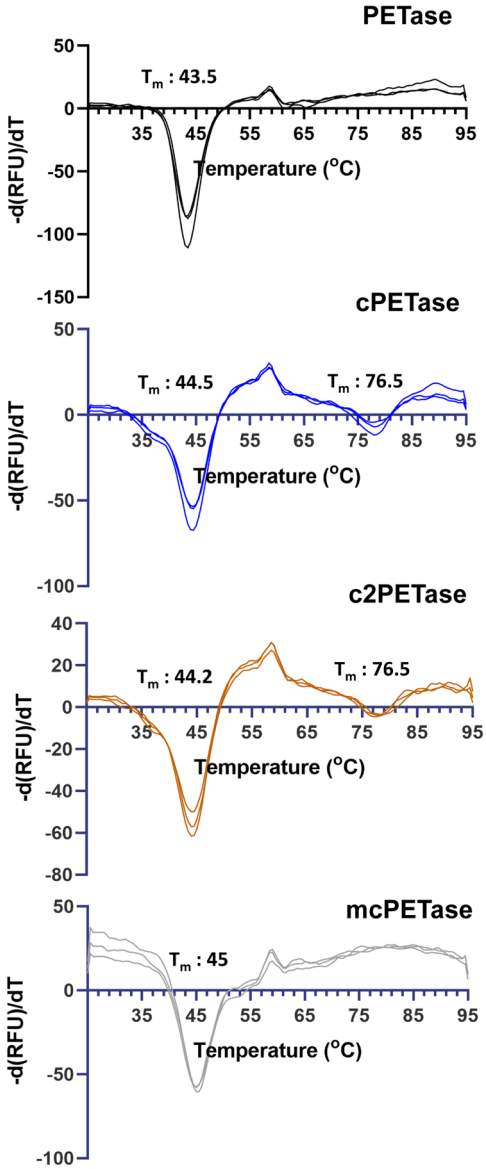

FIGURE 3 Fluorescence melt curve assays of PETase (black), cPETase (blue), c2PETase (orange), and mcPETase (gray). Each enzyme analyzed in triplicate. Calculated T_ms indicated.

TABLE 1 Kinetic parameters of PETase, cPETase, and c2PETase measured using PNPA as substrate. $n = 2 \pm SD$.

Enzyme	K_m (mM)	k_{cat} (s^{-1})	k_{cat}/K_m (s^{-1} mM^{-1})
PETase	1.98 ± 0.10	11.14 ± 0.68	5.63 ± 0.05
cPETase	4.8 ± 0.32	2.86 ± 0.17	0.587 ± 0.003
c2PETase	0.73 ± 0.067	7.33 ± 0.82	10.08 ± 0.533

Abbreviations: PNPA, para nitrophenyl acetate; SD, standard deviation.

when inserted into the vGFP scaffold (60°C). In both constructs, a clear peak was observed at ~87°C. This derives from spectral overlap of eGFP fluorescence measured in the channel used to detect SYPRO orange for the thermofluor assay, and corresponds to the T_m of the

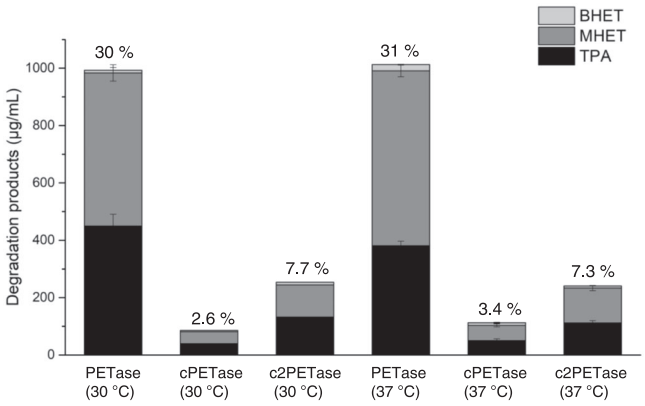

FIGURE 4 lcPET 1445 powder degradation by PETase and c/c2PETase. Reactions were incubated for 3 days at indicated temperatures and degradation products quantified. Numbers above indicate percentage of PET degraded. BHET, bis(2-hydroxyethyl) terephthalate; MHET, mono-(2-hydroxyethyl) terephthalate; TPA, terephthalic acid. $n = 2 \pm SD$.

vGFP chromophore. This was confirmed by analyzing vGFP-PETase and control linear eGFP-PETase using intrinsic GFP fluorescence as a reporter of stability (Chee et al., 2021) (Figure 7b). Clear differences in the melt profiles were observed, with fluorescence of eGFP-PETase starting to decline at ~50°C compared to ~76°C for vGFP-PETase. The terminal peak at 89°C for both proteins corresponded to the T_m of the vGFP chromophore.

Activity of vGFP-PETase on PET substrate was only very slightly reduced compared to PETase (Figure 8). This result contrasts with the SC-ST cyclized C2PETase variant, where a significant reduction in activity was observed (Figure 4). As expected, FAST showed superior activity over PETase (~2.5 fold). vGFP-FAST PET degradation was the same as for FAST, again indicating no major compromise of activity due to scaffolding approach used.

The measured T_ms of the scaffolded PETase component in all the constructs were similar to that of linear PETase. However, residual activity and solubility analysis postheating indicated clear gains in thermostability (Figures 2, 5, 7). To further address, CD analysis was carried out to measure protein folding. Stability was followed by measuring the 222 nm signal at elevated temperature (55°C) and remeasuring after cooling to 30°C (Figure 9, Supporting Information: Figures S4–S9). While no signal was observed for PETase at 55°C, both c1/c2PETase showed ~ 33% of control signal (nonheated sample). Furthermore, subsequent measurement after cooling to 30°C led to increased signals for both, this being more prominent for c2PETase (54.3%). These data are highly indicative of refolding promoted by the SC-ST scaffold. As a further control, we analyzed FAST PETase. This retained ~90% of its CD signal at 55°C, which is expected given its considerably higher T_m. vGFP-PETase and vGFP-FAST were also analyzed by CD, measuring signals at a further elevated temperature (80°C) given their superior thermostabilities (Figure 5). vGFP-PETase retained ~60% of control signal while vGFP-FAST retained ~89%, commensurate with the enhanced thermostability of the mutant PETase

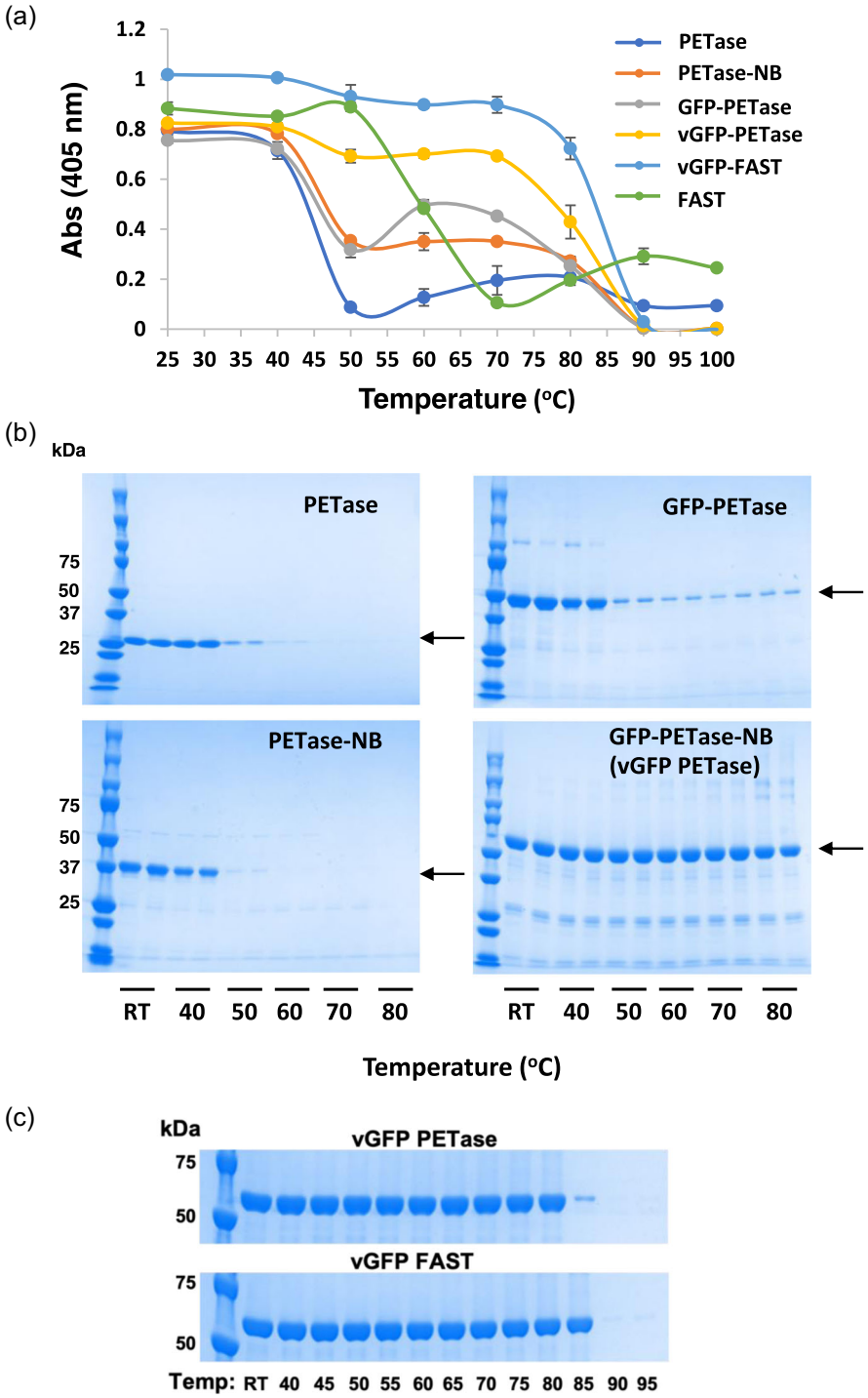

FIGURE 5 (a) Activity and thermostability of PETase, vGFP PETase, and indicated controls using para nitrophenyl acetate (PNPA) substrate. Enzymes (50 nM) were incubated at indicated temperatures for 10 min and PNPA hydrolysis measured. $n = 2 \pm$ SD. (b) Enzyme thermostability measured by SDS PAGE. Enzymes were incubated at indicated temperatures for 10 min and denatured/precipitated proteins removed by centrifugation. Soluble proteins were visualized by SDS PAGE ($n = 2$). (c) Same as in (b) for indicated enzymes (for repeat experiment see Supporting Information: Figure S3). RT, room temperature.

in the latter. As before, cooling led to signal gains, particularly for vGFP-PETase with ~82% of control signal being measured. As with SC-ST, vGFP is likely promoting refolding of the scaffolded PETase.

4 | DISCUSSION

We have generated thermostable versions of PETase using two scaffolding approaches. The first employed the orthogonal SC-ST pair that has been used to stabilize several other enzymes. While thermostability was achieved, linker length iterations were required to restore enzymatic activity on the model PNPA substrate. However, activity on PET substrate was still clearly compromised. This suggests either some form of steric hinderance arising from the SC and ST components that restricts efficient binding and/or restraint of essential protein dynamics required to tackle the bulkier insoluble PET substrate. Given that active site flexibility has been described as a hallmark of PET hydrolase enzymes (Fecker et al., 2018), the latter is a strong possibility. Additional linker length iterations will likely address this issue. Furthermore, the larger GFP and NB components

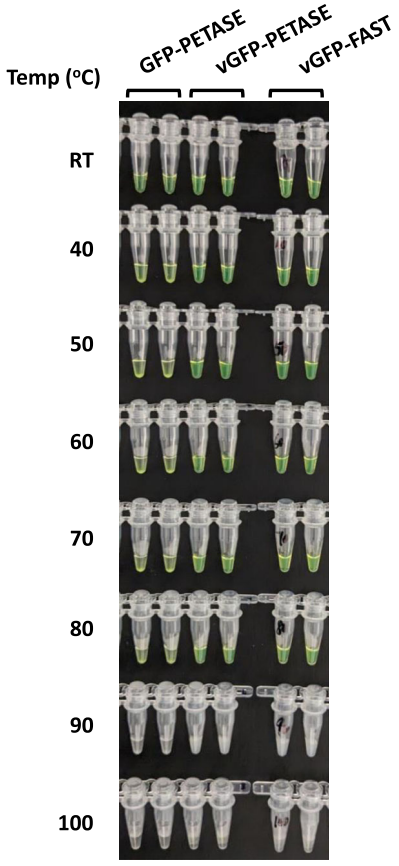

FIGURE 6 eGFP fluorescence of eGFP-PETase, vGFP-PETase, and vGFP-FAST imaged after 10 min incubation at indicated temperatures. Duplicate samples shown for each enzyme.

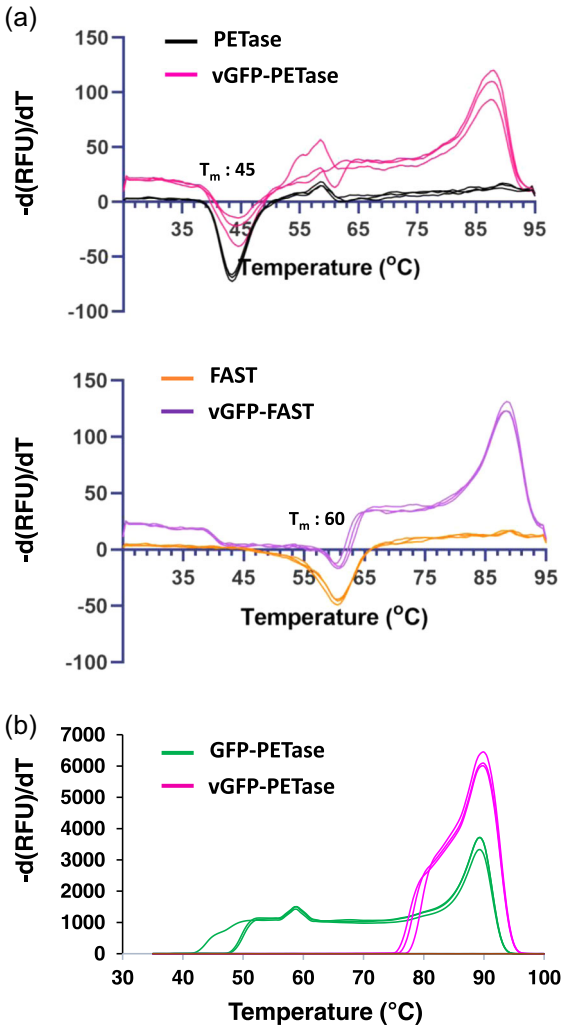

FIGURE 7 (a) Thermal melt curve assay using SYPRO indicator dye for PETase (black), vGFP-PETase (magenta), FAST (orange), and vGFP-FAST (purple). Triplicate data shown for each enzyme. Note the increase in signal at higher temperatures is due to spectral overlap from denaturation of the eGFP chromophore. (b) Thermal melt curve assays of eGFP-PETase and vGFP-PETase measured using intrinsic eGFP florescence. Triplicate data shown for each enzyme.

in the vGFP scaffold did not restrict activity on PET substrate, again suggesting compromise of essential active site dynamics on complex PET substrate. It was recently reported that SC-ST cyclization of PETase did not introduce thermostability (Hayes & Luk, 2023). Our results show thermostabilization based on activity, thermal precipitation assays and CD analysis. In agreement with the recent study, the T_m of the PETase component of the cyclized PETase was the same as for the linear wild-type PETase. Cyclization, therefore, promotes some degree of refolding as suggested by the CD analysis. Divergence between the studies most likely arises from the shorter linker previously used (14 residues in total) compared to this study (21 residues in cPETase and 26 in c2PETase). Notably, the additional five linker residues in c2PETase had a marked effect on PNPA hydrolysis compared to cPETase (17-fold increase in K_{cat}/k_m), highlighting the importance of linker length optimization.

Our next approach used the vGFP scaffold for the first time on a protein insert to introduce thermostability. The results showed clear thermostabilization of PETase that was readily measurable using the intrinsic GFP fluorescence. As with SC-ST scaffolding, the T_m of the PETase component in this scaffold did not increase. However, the data indicate that vGFP can both maintain solubility of the denatured PETase insert at temperatures significantly above its T_m and promote subsequent refolding after transitioning to lower temperatures. Both activity assays and CD analyses indicated a T_m of ~80°C for vGFP-PETase, and this was clearly higher for vGFP-FAST (85°C), making this construct the most thermostable PETase variant disclosed thus far. In contrast to SC-ST cyclization, the thermostable vGFP construct tested did not show repressed activity on PET substrate. Furthermore, improved activity of the FAST PETase variant on PET was maintained in the vGFP scaffold. The effective unstructured linker length in vGFP-PETase is 23 amino acids (21 from insertion, two from unstructured C-terminus of eGFP), shorter than the 29 and 34 residues for c/c2PETase respectively (including eight unstructured residues at C-terminus of SC (Li et al., 2014)). Topological differences, therefore, likely account for the observed differences in activity of PETase inserted into the scaffolds, with future structural analyses being key to understanding.

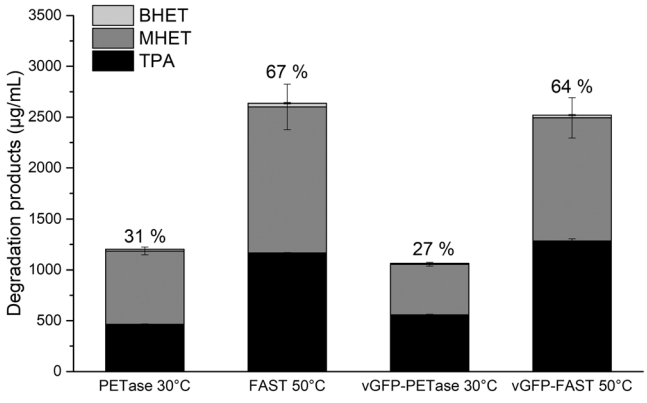

FIGURE 8 IcPET 1445 powder degradation by indicated enzymes. Reactions were incubated for 3 days at indicated temperatures and degradation products quantified. Numbers above indicate percentage of PET degraded. BHET, bis(2-hydroxyethyl) terephthalate; MHET, mono-(2-hydroxyethyl) terephthalate; TPA, terephthalic acid. $n = 2 \pm SD$.

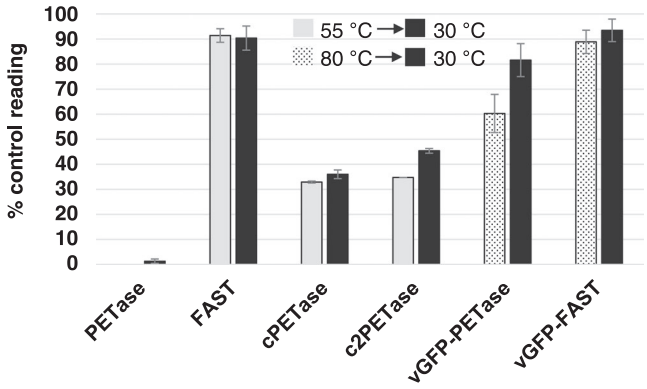

FIGURE 9 Thermal stability of PETase and variants measured by circular dichroism. Unfolding was determined by measuring the signal at 222 nm at indicated temperatures (55, 80°C) and remeasuring after cooling down to 30°C. Values shown as percentage signal for nonheat-treated control (measured at 30°C).

With a T_m of 80°C, thermostable vGFP-PETase represents an ideal departure point for engineering campaigns as it should both inherently be tolerable to extensive mutation, that is, more evolvable (Bloom et al., 2006), and its intrinsic GFP fluorescence can be used to normalize expression levels when libraries are screened. Furthermore, the linker regions potentially offer modular engineering options to introduce functionality, for example, charge modifications that may impact substrate binding (Nakamura et al., 2021).

AUTHOR CONTRIBUTIONS

Barindra Sana, Ke Ding, Jia Wei Siau, Rupali Reddy Pasula, Sharon Chee, Sharad Kharel, Jean-Baptise Henri Lena, Eunice Goh: Carried out experiments. **Lakshminarayanan Rajamani, Yeng Ming Lam, Sierin Lim, and John F. Ghadessy**: supervised/conceived experiments. **John F. Ghadessy**: Wrote the manuscript. All authors reviewed and edited the manuscript.

ACKNOWLEDGMENTS

This work was funded by the National Research Foundation, Singapore (NRF-CRP22-2019-0005).

CONFLICT OF INTEREST STATEMENT

The authors declare no conflict of interest.

DATA AVAILABILITY STATEMENT

The data that support the findings of this study are available from the corresponding author upon reasonable request.

ORCID

John F. Ghadessy http://orcid.org/0000-0001-8559-903X

REFERENCES

Austin, H. P., Allen, M. D., Donohoe, B. S., Rorrer, N. A., Kearns, F., Silveira, R. L., Pollard, B., Dominick, G., Duman, R., Omari, K. E., Mikhailik, V. B., Wagner, A., Michener, W. E., Amore, A., Skaf, M. S., Crowley, M. F., Thorne, A. W., Johnson, C., Woodcock, H. L. … Beckham, G. T. (2018). Characterization and engineering of a plastic-degrading aromatic polyesterase. *Proceedings of the National Academy of Sciences of the United States of America*, *115*, E4350–E4357.

Bell, E. L., Smithson, R., Kilbride, S., Foster, J., Hardy, F. J., Ramachandran, S., Tedstone, A. A., Haigh, S. J., Garforth, A. A., Day, P. J. R., Levy, C., Shaver, M. P., & Green, A. P. (2022). Directed evolution of an efficient and thermostable PET depolymerase. *Nature Catalysis*, *5*, 673–681.

Bloom, J. D., Labthavikul, S. T., Otey, C. R., & Arnold, F. H. (2006). Protein stability promotes evolvability. *Proceedings of the National Academy of Sciences*, *103*, 5869–5874.

Chee, S. M. Q., Wongsantichon, J., Yi, L. S., Sana, B., Frosi, Y., Robinson, R. C., & Ghadessy, F. J. (2021). Functional display of bioactive peptides on the vGFP scaffold. *Scientific Reports*, *11*, 10127.

Cui, Y., Chen, Y., Liu, X., Dong, S., Tian, Y., Qiao, Y., Mitra, R., Han, J., Li, C., Han, X., Liu, W., Chen, Q., Wei, W., Wang, X., Du, W., Tang, S., Xiang, H., Liu, H., Liang, Y., Houk, K. N., & Wu, B. (2021). Computational redesign of a PETase for plastic biodegradation under ambient condition by the GRAPE strategy. *ACS Catalysis*, *11*, 1340–1350.

Eshaghi, M., Sun, G., Grüter, A., Lim, C. L., Chee, Y. C., Jung, G., Jauch, R., Wohland, T., & Chen, S. L. (2015). Rational structure-based design of bright GFP-based complexes with tunable dimerization. *Angewandte Chemie International Edition*, *54*, 13952–13956.

Fecker, T., Galaz-Davison, P., Engelberger, F., Narui, Y., Sotomayor, M., Parra, L. P., & Ramírez-Sarmiento, C. A. (2018). Active site flexibility as a hallmark for efficient PET degradation by I. sakaiensis PETase. *Biophysical Journal*, *114*, 1302–1312.

Hayes, H. C., & Luk, L. Y. P. (2023). Investigating the effects of cyclic topology on the performance of a plastic degrading enzyme for polyethylene terephthalate degradation. *Scientific Reports*, *13*, 1267.

Itim, B., & Philip, M. (2015). Effect of multiple extrusions and influence of PP contamination on the thermal characteristics of bottle grade recycled PET. *Polymer Degradation and Stability*, *117*, 84–89.

Joho, Y., Vongsouthi, V., Spence, M. A., Ton, J., Gomez, C., Tan, L. L., Kaczmarski, J. A., Caputo, A. T., Royan, S., Jackson, C. J., & Ardevol, A. (2023). Ancestral sequence reconstruction identifies structural changes underlying the evolution of *Ideonella sakaiensis* PETase and variants with improved stability and activity. *Biochemistry*, *62*, 437–450.

Joo, S., Cho, I. J., Seo, H., Son, H. F., Sagong, H.-Y., Shin, T. J., Choi, S. Y., Lee, S. Y., & Kim, K.-J. (2018). Structural insight into molecular mechanism of poly (ethylene terephthalate) degradation. *Nature Communications*, *9*, 382.

Kawai, F., Oda, M., Tamashiro, T., Waku, T., Tanaka, N., Yamamoto, M., Mizushima, H., Miyakawa, T., & Tanokura, M. (2014). A novel Ca2+-activated, thermostabilized polyesterase capable of hydrolyzing polyethylene terephthalate from Saccharomonospora viridis AHK190. *Applied Microbiology and Biotechnology*, *98*, 10053–10064.

Kijo-Kleczkowska, A., & Gnatowski, A. (2022). Recycling of plastic waste, with particular emphasis on thermal methods—review. *Energies*, *15*, 2114.

Lau, S. Y., Siau, J. W., Sobota, R. M., Wang, C. I., Zhong, P., Lane, D. P., & Ghadessy, F. J. (2018). Synthetic 10FN3-based mono- and bivalent inhibitors of MDM2/X function. *Protein Engineering, Design and Selection*, *31*, 301–312.

Li, L., Fierer, J. O., Rapoport, T. A., & Howarth, M. (2014). Structural analysis and optimization of the covalent association between SpyCatcher and a peptide tag. *Journal of Molecular Biology*, *426*, 309–317.

Liu, B., He, L., Wang, L., Li, T., Li, C., Liu, H., Luo, Y., & Bao, R. (2018). Protein crystallography and site-direct mutagenesis analysis of the poly(ethylene terephthalate) hydrolase PETase from *Ideonella sakaiensis*. *ChemBioChem*, *19*, 1471–1475.

Lu, H., Diaz, D. J., Czarnecki, N. J., Zhu, C., Kim, W., Shroff, R., Acosta, D. J., Alexander, B. R., Cole, H. O., Zhang, Y., Lynd, N. A., Ellington, A. D., & Alper, H. S. (2022). Machine learning-aided engineering of hydrolases for PET depolymerization. *Nature*, *604*, 662–667.

Matulis, D., Kranz, J. K., Salemme, F. R., & Todd, M. J. (2005). Thermodynamic stability of carbonic anhydrase: measurements of binding affinity and stoichiometry using ThermoFluor. *Biochemistry*, *44*, 5258–5266.

Meng, X., Yang, L., Liu, H., Li, Q., Xu, G., Zhang, Y., Guan, F., Zhang, Y., Zhang, W., Wu, N., & Tian, J. (2021). Protein engineering of stable IsPETase for PET plastic degradation by premuse. *International Journal of Biological Macromolecules*, *180*, 667–676.

Müller, R.-J., Schrader, H., Profe, J., Dresler, K., & Deckwer, W.-D. (2005). Enzymatic degradation of poly(ethylene terephthalate): rapid hydrolyse using a hydrolase from T. fusca. *Macromolecular Rapid Communications*, *26*, 1400–1405.

Nakamura, A., Kobayashi, N., Koga, N., & Iino, R. (2021). Positive charge introduction on the surface of thermostabilized PET hydrolase facilitates PET binding and degradation. *ACS Catalysis*, *11*, 8550–8564.

Rennison, A., Winther, J. R., & Varrone, C. (2021). Rational protein engineering to increase the activity and stability of IsPETase using the PROSS algorithm. *Polymers*, *13*, 3884.

Rochman, C. M., Browne, M. A., Halpern, B. S., Hentschel, B. T., Hoh, E., Karapanagioti, H. K., Rios-Mendoza, L. M., Takada, H., Teh, S., & Thompson, R. C. (2013). Classify plastic waste as hazardous. *Nature*, *494*, 169–171.

Samak, N. A., Jia, Y., Sharshar, M. M., Mu, T., Yang, M., Peh, S., & Xing, J. (2020). Recent advances in biocatalysts engineering for polyethylene terephthalate plastic waste green recycling. *Environment International*, *145*, 106144.

Sana, B., Chee, S. M. Q., Wongsantichon, J., Raghavan, S., Robinson, R. C., & Ghadessy, F. J. (2019). Development and structural characterization of an engineered multi-copper oxidase reporter of protein-protein interactions. *Journal of Biological Chemistry*, *294*, 7002–7012.

Schoene, C., Fierer, J. O., Bennett, S. P., & Howarth, M. (2014). SpyTag/SpyCatcher cyclization confers resilience to boiling on a mesophilic enzyme. *Angewandte Chemie International Edition*, *53*, 6101–6104.

Shi, L., Liu, P., Tan, Z., Zhao, W., Gao, J., Gu, Q., Ma, H., Liu, H., & Zhu, L. (2023). Complete depolymerization of PET wastes by an evolved PET hydrolase from directed evolution. *Angewandte Chemie International Edition*, *62*, e202218390.

Si, M., Xu, Q., Jiang, L., & Huang, H. (2016). SpyTag/SpyCatcher cyclization enhances the thermostability of firefly luciferase. *PLoS One*, *11*, e0162318.

Siau, J. W., Nonis, S., Chee, S., Koh, L. Q., Ferrer, F. J., Brown, C. J., & Ghadessy, F. J. (2020). Directed co-evolution of interacting protein-peptide pairs by compartmentalized two-hybrid replication (C2HR). *Nucleic Acids Research*, *48*, e128.

Son, H. F., Cho, I. J., Joo, S., Seo, H., Sagong, H. Y., Choi, S. Y., Lee, S. Y., & Kim, K. J. (2019). Rational protein engineering of thermo-stable PETase from *Ideonella sakaiensis* for highly efficient PET degradation. *ACS Catalysis*, *9*, 3519–3526.

Son, H. F., Joo, S., Seo, H., Sagong, H. Y., Lee, S. H., Hong, H., & Kim, K. J. (2020). Structural bioinformatics-based protein engineering of thermo-stable PETase from *Ideonella sakaiensis*. *Enzyme and Microbial Technology*, *141*, 109656.

Sulaiman, S., Yamato, S., Kanaya, E., Kim, J. J., Koga, Y., Takano, K., & Kanaya, S. (2012). Isolation of a novel cutinase homolog with polyethylene terephthalate-degrading activity from leaf-branch compost by using a metagenomic approach. *Applied and Environmental Microbiology*, *78*, 1556–1562.

Thiyagarajan, S., Maaskant-Reilink, E., Ewing, T. A., Julsing, M. K., & van Haveren, J. (2022). Back-to-monomer recycling of polycondensation polymers: Opportunities for chemicals and enzymes. *RSC Advances*, *12*, 947–970.

Tournier, V., Topham, C. M., Gilles, A., David, B., Folgoas, C., Moya-Leclair, E., Kamionka, E., Desrousseaux, M. L., Texier, H., Gavalda, S., Cot, M., Guémard, E., Dalibey, M., Nomme, J., Cioci, G., Barbe, S., Chateau, M., André, I., Duquesne, S., & Marty, A. (2020). An engineered PET depolymerase to break down and recycle plastic bottles. *Nature*, *580*, 216–219.

Wang, J., Wang, Y., Wang, X., Zhang, D., Wu, S., & Zhang, G. (2016). Enhanced thermal stability of lichenase from Bacillus subtilis 168 by SpyTag/SpyCatcher-mediated spontaneous cyclization. *Biotechnology for Biofuels*, *9*, 79.

Woodman, R., Yeh, J. T. H., Laurenson, S., & Ferrigno, P. K. (2005). Design and validation of a neutral protein scaffold for the presentation of peptide aptamers. *Journal of Molecular Biology*, *352*, 1118–1133.

Yin, Q., You, S., Zhang, J., Qi, W., & Su, R. (2022). Enhancement of the polyethylene terephthalate and mono-(2-hydroxyethyl) terephthalate degradation activity of *Ideonella sakaiensis* PETase by an electrostatic interaction-based strategy. *Bioresource Technology*, *364*, 128026.

Yoshida, S., Hiraga, K., Takehana, T., Taniguchi, I., Yamaji, H., Maeda, Y., Toyohara, K., Miyamoto, K., Kimura, Y., & Oda, K. (2016). A bacterium that degrades and assimilates poly(ethylene terephthalate). *Science*, *351*, 1196–1199.

Zakeri, B., Fierer, J. O., Celik, E., Chittock, E. C., Schwarz-Linek, U., Moy, V. T., & Howarth, M. (2012). Peptide tag forming a rapid covalent bond to a protein, through engineering a bacterial adhesin. *Proceedings of the National Academy of Sciences*, *109*, E690.

Zurier, H. S., & Goddard, J. M. (2023). A high-throughput expression and screening platform for applications-driven PETase engineering. *Biotechnology and Bioengineering*, *120*, 1000–1014.

SUPPORTING INFORMATION

Additional supporting information can be found online in the Supporting Information section at the end of this article.

How to cite this article: Sana, B., Ding, K., Siau, J. W., Pasula, R. R., Chee, S., Kharel, S., Lena, J.-B., Goh, E., Rajamani, L., Lam, Y. M., Lim, S., & Ghadessy, J. F. (2023). Thermostability enhancement of polyethylene terephthalate degrading PETase using self- and nonself-ligating protein scaffolding approaches. *Biotechnology and Bioengineering*, *120*, 3200–3209. https://doi.org/10.1002/bit.28523